Stability of densely branched growth in dissipative diffusion-controlled systems

Juan K. Lin and David G. Grier
Department of Physics and James Franck Institute, The University of Chicago, 5640 S. Ellis Avenue, Chicago, Illinois 60637
(Received 22 November 1995; revised manuscript received 16 May 1996)

The dense branching morphology appears in a number of pattern-forming systems. Neither ordered nor fractal, this pattern is characterized by a large number of branches advancing at constant areal density behind a smooth envelope. We propose a two-sided model which accounts for the stability of the dense branching morphology (DBM) through dissipative and anisotropic current transport in the evolving pattern. Confinement of currents to slightly resistive branches suffices to stabilize radially symmetric DBM growth in two and three dimensions. Stability of the planar DBM, on the other hand, is found to require, in addition, the introduction of a characteristic length scale, such as a short diffusion length. [S1063-651X(96)03009-7]

PACS number(s): 68.70.+w, 47.54.+r, 68.35.Fx

I. INTRODUCTION

Several distinct classes of patterns, or morphologies, can emerge when the interface between two phases is driven out of equilibrium by a diffusive field. Highly branched fractals resembling diffusion limited aggregation (DLA) clusters [1], snowflakelike dendrites [2], and dense branching patterns [3,4] are produced by processes as varied as viscous fluid displacement and electrochemical deposition of metals and polymers. The dense branching morphology (DBM), examples of which appear in Fig. 1, is characterized by a large number of fine branches advancing behind a smooth stable envelope. Unlike ordered dendrites, the individual branches in the DBM are unstable against repeated tip splitting. In this respect, the DBM more closely resembles DLA. Unlike DLA, however, the ensemble of DBM branches fills space uniformly. The underlying interfacial instability responsible for branch formation also might be expected to destabilize the apparent interface enclosing the branch tips. A central challenge for models of densely branched growth, thus, is to explain the stability of the smooth advancing envelope.

Many pattern forming systems such as electrochemical deposition, viscous fingering, and dielectric breakdown can be described by a model in which the interface's movement is governed by a scalar field satisfying Laplace's equation at least in the quasistatic limit [5,6]. The simplest version of the Laplacian growth model treats the moving interface as an equipotential. Under these conditions, the tendency of protrusions to concentrate field gradients, which was first emphasized in this context by Mullins and Sekerka [7], renders a smooth advancing interface linearly unstable to perturbations at all wavelengths. Corrections to the interfacial potential due to surface tension and growth kinetics can stabilize the interface at wavelengths comparable to the width of a branch, but do not suppress longer-wavelength instabilities. Extension of the Mullins-Sekerka analysis to systems with finite diffusion lengths also results in linear instability at long wavelengths. The existence of these long-wavelength instabilities suggest that the DBM cannot form in standard nondissipative models for diffusive pattern formation.

Previous efforts [4,8,9] to extend these models by accounting for the small but nonvanishing resistance to gradient-driven currents in the patterns' branches have been obliged to distinguish between two experimental geometries. In the radial geometry the pattern grows outward from a source of radius r_c centered within a region of radius R, while in the flat geometry it advances between parallel planar boundaries separated by distance R. The distinction arises because the DBM was found to be linearly stable in the two-dimensional radial case, but not in the planar geometry [4]. Thus these models fail to account for the appearance of structures such as that in Fig. 1(b) which suggests that the DBM can occur in the planar geometry also.

This article is organized as follows. The growth model is presented in Sec. II in the context of pattern formation during electrochemical deposition and viscous fingering. This section also outlines the linear stability analysis used in the following section to investigate morphological stability of the DBM. The central results of this article are presented in Sec. III. Section III A reviews our previously reported results for the 2D radial geometry in the quasistationary approximation. We extend this analysis in Secs. III B and III C both to the 3D radial geometry and also beyond the quasistationary approximation in the planar geometry. We find a range of nontrivial growth conditions under which the radial DBM is linearly stable in three dimensions. No such conditions are found for growth from a line or a plane in the quasistationary approximation. Stability of the planar DBM is established, however, by including both dissipation and a finite diffusion length. This analysis therefore extends the range of pattern forming systems for which the dissipative growth model accounts for the appearance of the dense branching morphology.

II. DISSIPATIVE AND ANISOTROPIC GROWTH MODEL

Dissipation occurs naturally in the growth channels of many physical pattern forming systems. In electrochemical deposition, for example, the deposited metal has a measurable resistance; the advancing fluid in viscous fingering systems similarly has a finite viscosity. A complete theory for pattern formation in such systems would account for field gradients within the detailed branching geometry of the evolving pattern. In the absence of such a theory, we construct a self-consistent model by assuming that a dense branching pattern has already formed and investigating its

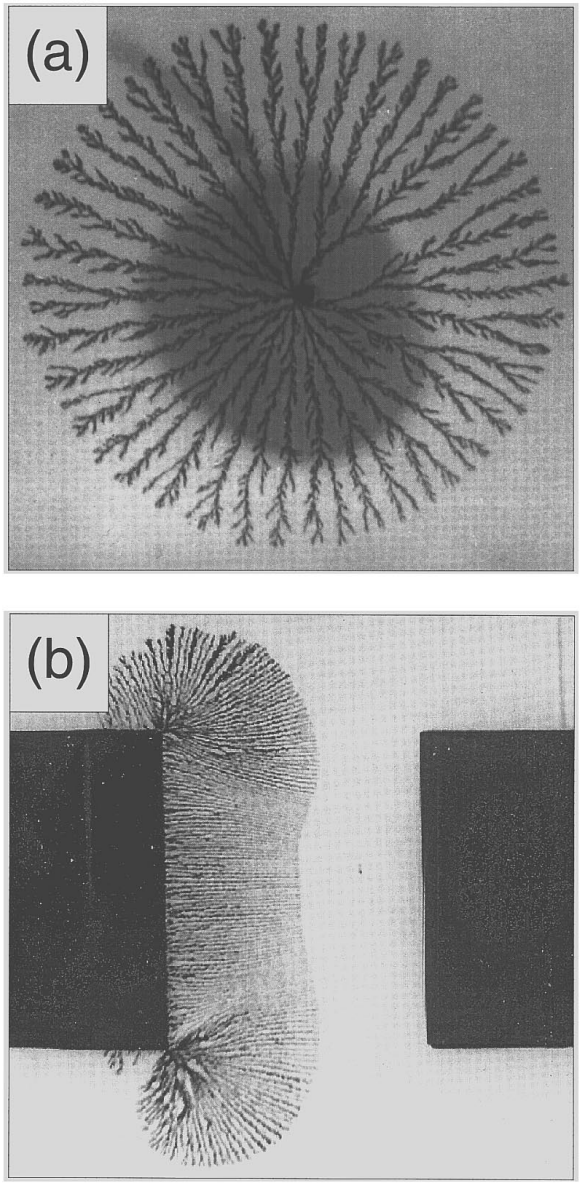

FIG. 1. Densely branched growth in quasi-two-dimensional electrochemical deposition. (a) Radial geometry. Zinc deposited from 0.05M $ZnSO_4$ at 10 V, with $r_c = 0.1$ mm and $R = 4.2$ cm. (b) Flat geometry. Copper deposited from 0.1M $CuSO_4$ at 5 V with $R = 4$ mm.

stability against small deformations. We treat the region behind the smooth advancing envelope as an effective medium whose transport properties mimic those of actual patterns at least in an average sense.

Our two-sided model consists of a scalar field both in the patterned aggregate region (region 1) and in the region outside (region 2). Within the aggregate region, the field $u_1(\vec{r})$ satisfies an anisotropic Laplace's equation

$$\sigma_{\parallel}\nabla_{\parallel}^2 u_1 + \sigma_{\perp}\nabla_{\perp}^2 u_1 = 0, \tag{1}$$

where $\sigma_{\parallel}$ and $\sigma_{\perp}$ are, respectively, the conductivities along and perpendicular to the branches; $\nabla_{\parallel}^2$ and $\nabla_{\perp}^2$ denote the corresponding components of the Laplacian. This macroscopic conductivity anisotropy originates from the branched structure of the DBM and reflects the currents' preference to flow along the branches rather than between them. It should not be confused with the microscopic crystalline anisotropy which is responsible for stabilizing the dendritic morphology against tip splitting.

Outside the pattern, we assume the field $u_2(\vec{r})$ satisfies the diffusion equation

$$\sigma_2 \nabla^2 u_2 = \frac{\partial u_2}{\partial t}. \tag{2}$$

This reduces to the usual Laplace's equation in the quasistatic limit. The conductivity σ_2 in this region is isotropic. We assume that the interface advances at a rate proportional to the local current density, $\vec{v} = b\vec{j}|_{\vec{r}_s}$, where b is a system-dependent material parameter and $\vec{r}_s$ is the position of the interface. We further assume that the currents arise from gradients in the field according to Fick's law

$$\vec{j} = \sigma \vec{\nabla} u. \tag{3}$$

The system is driven out of equilibrium by a constant potential difference applied across the boundaries at $\vec{r}_c$ and $\vec{R}$

$$u_1(\vec{r}_c) = 0, \tag{4}$$

and

$$u_2(\vec{R}) = 1. \tag{5}$$

Assuming continuity in both the field and current across the interface at $\vec{r}_s$,

$$u_1(\vec{r}_s) = u_2(\vec{r}_s), \tag{6}$$

and

$$\vec{j}_1(\vec{r}_s) = \vec{j}_2(\vec{r}_s) \tag{7}$$

allows us to solve for the interface's evolution.

In the context of electrochemical deposition, Eqs. (1)–(7) might be interpreted as describing a pair of arbitrarily shaped electrodes held at a fixed voltage difference in contact with an electrolyte of conductivity σ_2. The field $u(\vec{r})$ then would correspond roughly to the electrochemical potential at position $\vec{r}$. For viscous fingering, $u(\vec{r})$ represents the local pressure field, and the system is driven by a constant pressure difference between the boundaries. While this simple growth model glosses over most system-dependent details which might dominate a system's behavior under some operating conditions, its behavior is rich enough to shed light on generic mechanisms of pattern formation under diffusive control.

We find it useful to define two-dimensionless control parameters: the conductivity anisotropy

$$\gamma^2 = \frac{\sigma_{\perp}}{\sigma_{\parallel}}, \tag{8}$$

and the conductivity contrast

$$\beta = \frac{\sigma_2}{\sigma_{\parallel}}. \tag{9}$$

Large anisotropy is indicated by small values of γ, which physically correspond to stronger confinement of currents to the branches. Smaller values of β similarly correspond to stronger conductivity contrast between the invading and displaced phases. For viscous fingering, the condition $\beta>1$ corresponds to injecting a viscous fluid into an inviscid fluid. The interface is intrinsically stable under these conditions and no branches form. By contrast, $\beta=0$ corresponds to the DLA-like case in which the aggregate surface is an equipotential and the interface is intrinsically unstable at all wavelengths. We focus instead on the more interesting intermediate range $0<\beta<1$.

Analysis of this model can either proceed numerically on a computer, or analytically via linear stability analysis. Previously [4], 2D radial computer simulations of this model were performed, showing DLA and DBM-like growth. Here, we concentrate on linear stability analysis to probe the predictions of our model in various geometries. Following the procedure described by Mullins and Sekerka [7] we first assume that a radial or planar DBM has formed of a certain size and that its envelope separates regions 1 and 2 in the above formulation. The envelope is then distorted with a perturbation of infinitesimal amplitude δ. Since a general infinitesimal perturbation can be built up by linear superposition of any complete set of functions, we examine only sinusoidal modulations in the 2D radial and planar geometries, and spherical harmonics in the 3D radial geometry. The response of the system to linear order in δ is then calculated in the form of a dimensionless growth rate of the perturbation

$$\alpha=\frac{\dot{\delta}/\delta}{v_0/r_0}, \tag{10}$$

where r_0 labels the position of the unperturbed envelope, and v_0 its velocity.

III. RESULTS

A. Two-dimensional radial geometry

In the two-dimensional radial geometry, a DBM aggregate has a circular envelope of radius r_0 with radially radiating branches. We have discussed this geometry in detail in Ref. [4] and include an overview here for completeness and to contrast with results for other geometries. A circular interface preserves its shape under Eqs. (1)–(7) and advances with a radial velocity

$$v_0=\frac{b\sigma_2}{r_0\left[\beta\,\ln\left(\frac{r_0}{r_c}\right)+\ln\left(\frac{R}{r_0}\right)\right]}. \tag{11}$$

The conductivity anisotropy γ does not appear in Eq. (11) because there are no tangential currents in this radially symmetric solution. The linear stability of the interface is determined by studying the evolution of an m-fold sinusoidal perturbation of infinitesimal amplitude δ_m

$$r_s=r_0+\delta_m\cos(m\theta). \tag{12}$$

As we previously reported [4], the relative growth rate of perturbations in this model is

$$\alpha_m=-1+\frac{m\gamma(1-\beta)}{\beta\,\tanh\left[m\gamma\,\ln\left(\frac{r_0}{r_c}\right)\right]+\gamma\,\tanh\left[m\,\ln\left(\frac{R}{r_0}\right)\right]}. \tag{13}$$

This result was found to be in good qualitative and fair quantitative agreement with both numerical simulations and quasi-two-dimensional electrochemical deposition experiments.

For sufficiently large internal dissipation (values of β larger than zero) and sufficiently strong anisotropy (small values of γ), the relative growth rate is negative for small mode numbers; the circular envelope is stable against long-wavelength perturbations under these conditions. Both dissipation and current confinement are required to stabilize the smooth envelope of densely branched structures. In contrast to the suggestion of Erlbacher, Searson, and Sieradzki [10] that the dense branching morphology is stabilized in quasi-two-dimensional experiments by three-dimensional effects, our result indicates that the DBM can be stable in purely two-dimensional systems.

Earlier one-sided models which attempted to account for dissipation in the growth channels through corrections to the interfacial boundary condition failed to account for stable dense branching structures in electrochemical deposition when reasonable estimates for β were used [4,9,11]. Even with a conductivity contrast as small as $\beta\approx 1/100$, the present model can account for the stability of the DBM provided the confinement of currents to the branches is sufficiently strong. Comparable values for β have been estimated from measurements in quasi-two-dimensional electrochemical deposition experiments under conditions which formed the DBM [9]. Strong confinement of currents to the branches in these experiments is reasonable since the electrolyte between the branches is known to be largely depleted of metal ions [12].

B. Three-dimensional radial geometry

Experiments such as those depicted in Fig. 1 have three-dimensional analogs which have been studied [13–15] almost as extensively as their more easily interpreted two-dimensional variants. Recent advances in admittance spectroscopy [14] and image analysis [15] make it possible to analyze the shapes of evolving three-dimensional patterns. High speed magnetic resonance imaging also has been applied to the study of fluid flow in porous media. Three-dimensional radial pattern formation, in which branches grow outward from the end of a conduit, constitute another class of systems to which our growth model should pertain.

In the full three-dimensional radial geometry model, the unperturbed spherical interface advances with velocity

$$v_0=\frac{b\sigma_2}{r_0}\left[\frac{\beta r_0}{r_c}+(1-\beta)-\frac{r_0}{R}\right]^{-1}. \tag{14}$$

An infinitesimal perturbation to the growth front with a spherical harmonic

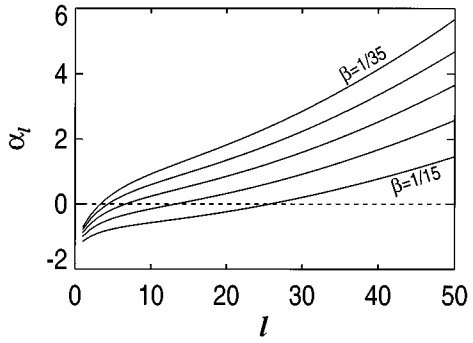

FIG. 2. Dimensionless growth rate α_l of the lth harmonic in the three-dimensional radial geometry. Conductivity anisotropy $\gamma=0.01$, $r_0=10r_c$, and $R=100r_c$. Lines are plotted for $\beta=\frac{1}{35}, \frac{1}{30}, \frac{1}{25}, \frac{1}{20}$, and $\frac{1}{15}$. As the branches become increasingly resistive, the critical mode number below which all modes are stable increases. The dependence on R is very weak provided $r_0 \ll R$.

$$r_s = r_0 + \delta_l^m Y_l^m(r,\theta,\phi) \tag{15}$$

grows at the relative rate

$$\alpha_l = -2 + (1-\beta)\left\{ \frac{2}{(2l+1)\coth\left[\frac{2l+1}{2}\ln\left(\frac{R}{r_0}\right)\right]+1} + \frac{2\beta}{w\,\coth\left[\frac{w}{2}\ln\left(\frac{r_0}{r_c}\right)\right]-1} \right\}^{-1}, \tag{16}$$

where $w=\sqrt{1+4\gamma^2 l(l+1)}$. Figure 2 shows a plot of the growth rate as a function of the perturbation harmonic for a range of dissipation values. The growth rate is negative for values of l less than a critical mode number l_c which depends on the degree of dissipation in the growth channels. Such long-wavelength perturbations shrink as the aggregate grows. The greater l_c, therefore, the more nearly spherical the evolving pattern appears. In Fig. 3 this marginally stable harmonic number is plotted as a function of the amount of dissipation (β) and anisotropy (γ) in the system. As seen from the plot, dissipation and current confinement act in concert to stabilize the dense branching morphology in the three-dimensional radial geometry.

In the limit $R \gg r_0$, we can solve for the critical aggregate radius beyond which the envelope will be stable against perturbations of harmonic number l

$$r_0^* = r_c\left[\frac{4\beta(l+1)+(1-\beta)(l+1)(w+1)-2(w+1)}{4\beta(l+1)-(1-\beta)(l+1)(w-1)+2(w-1)}\right]^{1/w}. \tag{17}$$

In the anisotropic limit ($\gamma \to 0$), the expression simplifies to

$$r_0^* = \left[1+\frac{1-\beta}{2\beta}-\frac{1}{\beta(l+1)}\right] r_c. \tag{18}$$

For $r_0^* < r_c$ the DBM is stable against perturbations of harmonic number greater than l. Even for $r_0^* > r_c$, an initially disordered core pattern can cross over into a regime where densely branched growth will be stable, provided the envelope equipotential still is reasonably smooth by the time the interface has advanced to a mean position $r=r_0^*$. The size at which the envelope of the growing pattern becomes stable scales with the size of the inner boundary r_c and depends strongly on the amount of dissipation in the system. The position at which such a crossover to stable dense radial growth might occur for $\gamma=1/100$ and $R=100r_c$ appears in Fig. 4 as a rapid increase in l_c with r_0. Under certain conditions, l_c decreases again for r_0 very near R and a second crossover from stable DBM to unstable growth is possible.

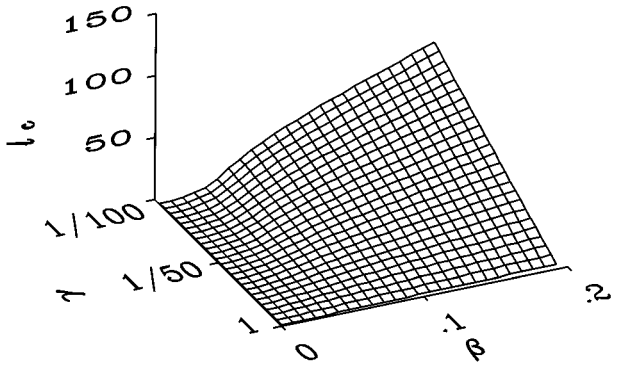

FIG. 3. Plot of the critical perturbation harmonic l_c as a function of the amount of dissipation β and degree of anisotropy γ in the three-dimensional radial geometry model, with $r_0=10r_c$, and $R=100r_c$. Dissipation and anisotropy both help stabilize the DBM.

C. Growth from a line or plane

In a planar geometry version of the dissipative quasistatic model, the growth rate of a sinusoidal perturbation of wave number k is given by

$$\alpha_k = \frac{kx_0(1-\beta)}{\frac{\beta}{\gamma}\tanh(\gamma k x_0)+\tanh[k(R-x_0)]}, \tag{19}$$

where x_0 is the location of the unperturbed interface along the growth direction $\hat{x}$. The growth rate α_k is positive for all wave numbers in all regions of parameter space, so that the flat envelope is unstable against perturbations at all wavelengths. This result reflects the planar geometry's lack of a characteristic length scale to play the role played by r_c in the radial geometry. Without such a reference against which to distinguish perturbations of different sizes, they are either all stable or all unstable. The branches' transport properties as modeled in Eq. (1) do not introduce new length scales themselves.

The quasistatic approximation to Eq. (2) requires the diffusion length $\lambda=\sigma_2/2v_0$ to be larger than any other characteristic sizes in the system. If we relax this requirement, then λ may influence the stability of the DBM. Thus outside the patterned aggregate region we seek a solution to the diffusion equation. The similarity transform $z=x/x_0(t)$ rescales the problem into the frame moving with the interface. In this frame, the diffusion equation has the form

$$\frac{d^2\overline{u_2}(z)}{dz^2} = -\xi\frac{d\overline{u_2}(z)}{dz}, \tag{20}$$

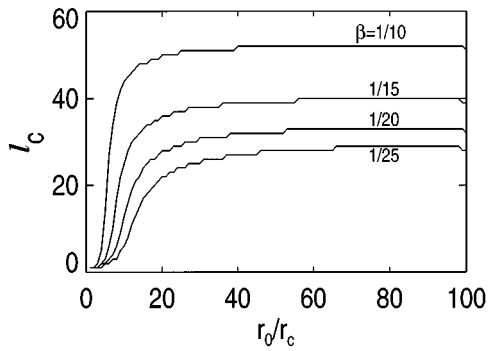

FIG. 4. Plot of the critical perturbation harmonic l_c as a function of the size of the pattern, r_0/r_c, in the three-dimensional radial geometry model, with $\gamma=0.01$ and $R=100r_c$. Lines are plotted for $\beta=\frac{1}{10}$, $\frac{1}{15}$, $\frac{1}{20}$, and $\frac{1}{25}$. Predictions for the size-dependent crossover to stable growth in the anisotropic limit given by Eq. (18), $r_0^*/r_c=5.5$, 8, 10.5, and 13 for the four β values, respectively, agree well with the jump in l_c for the full solution.

where $\overline{u_2}(z)=u_2(x,t)$ and $\xi=x_0v_0/\sigma_2$. Equation (20) is integrable provided that ξ is a constant. This requirement in turn determines the time dependence of the interfacial position and velocity

$$x_0=\sqrt{2\xi\sigma_2 t}, \tag{21}$$

and

$$v_0=\left(\frac{\xi\sigma_2}{2t}\right)^{1/2}.$$

Similar time evolution was obtained by Zener in his model of nondissipative diffusive growth [16]. The solution to Eq. (20) which satisfies the boundary conditions in Eqs. (5)–(7) in the limit of large R is given by

$$u_2(x,t)=\frac{\xi\beta}{b}+\left(1-\frac{\xi\beta}{b}\right)\left[1-\frac{\mathrm{erfc}(x/2\sqrt{\sigma_2 t})}{\mathrm{erfc}(\sqrt{\xi/2})}\right], \tag{22}$$

where ξ satisfies the transcendental equation

$$\exp\left(\frac{\xi}{2}\right)\mathrm{erfc}\left(\left[\frac{\xi}{2}\right]^{1/2}\right)=\left(\frac{2}{\pi\xi}\right)^{1/2}(b-\xi\beta). \tag{23}$$

We are now in a position to show that diffusion without dissipation in the growth channels is not sufficient to stabilize the planar DBM. In the limit $\beta=0$, the advancing pattern is an equipotential with $u_1(\vec{r}_s,t)=0$ and the linear stability calculation for the similarity solution gives

$$\alpha_k=kx_0>0. \tag{24}$$

Surprisingly this is the same result as was obtained by Mullins and Sekerka in the quasistatic limit [7]. Although the actual growth rate $\dot{\delta}$ depends on the diffusion length, the nondimensional growth rate does not.

Including contributions from dissipation and current confinement in the advancing region requires $u_2(\vec{r})$ to satisfy continuity conditions with the field inside,

$$u_1(x,t)=\frac{\xi\beta x}{bx_0} \tag{25}$$

at the interface. As before, we perturb the flat interface with a sinusoid of wave number k and solve for the growth rate of the perturbation to linear order in the perturbation's amplitude. The linear stability calculations then give

$$\alpha_k=\frac{qx_0(1-\beta)-\xi}{\frac{\beta q}{\gamma k}\tanh[\gamma k x_0]+1}, \tag{26}$$

where

$$qx_0=\frac{\xi}{2}+\left[\left(\frac{\xi}{2}\right)^2+(kx_0)^2+\alpha_k\xi\right]^{1/2}. \tag{27}$$

Equations (26) and (27) reduce to the dissipative Laplacian result [Eq. (19)] and nondissipative short diffusion length result [Eq. (24)] in the limits $\xi\to 0$, and $\beta\to 0$, respectively. These equations also can be solved for α_k, although the result is messy and so not particularly informative. For the sake of clarity, we leave the solution as two coupled equations which we can compare more easily with results from the earlier analyses.

In the limit that α_k is small compared with ξ, q plays the role of a wave number whose lower limit is set by the diffusion length $q>1/2\lambda$. This is the length scale against which features in the evolving pattern can be compared. The factor of β in the numerator of Eq. (26) then provides the offset necessary to achieve negative values of α_k and thus stability at long wavelengths.

Setting $\alpha_k=0$ in Eqs. (26) and (27) allows us to solve for the marginally stable mode number

$$k_c=\frac{\xi\sqrt{\beta}}{x_0(1-\beta)}. \tag{28}$$

Long-wavelength modes with $k<k_c$ are stable while modes with $k>k_c$ grow unstably; this is consistent with the overall picture of a large number of branches advancing behind a smooth envelope. The critical mode number depends inversely on the diffusion length λ through the constant $\xi=x_0/2\lambda$. Since the diffusion length changes as the pattern advances, however, ξ is a more useful control parameter.

It is noteworthy that the conductivity anisotropy γ does not influence k_c in the planar geometry despite its significant role in determining l_c in the radial geometry (see Fig. 3). The extent r_c of the central boundary condition sets the characteristic scale for quasistationary growth in the radial geometry and couples to the growth front through the pattern's transport properties. The diffusion length λ on the other hand, sets the scale of the problem outside the advancing interface and its influence depends only indirectly on the disposition of currents within the pattern.

Finally, it would appear from Eq. (28) that DBM growth is inevitable in the planar geometry since k_c diverges when $x_0=0$. In fact, the initial transient behavior at the onset of growth is not treated by Eq. (22) and thus is not accounted for in Eq. (28). Furthermore, the value for β may evolve as the morphology of the aggregate changes during early

growth, and this evolution will affect the interface's stability. The above analysis simply provides a mechanism by which the planar DBM, once formed, can be linearly stable. This analysis also demonstrates that the planar DBM must eventually become unstable since the critical mode number vanishes as the interface advances.

IV. CONCLUSIONS

The previous sections demonstrate that diffusive pattern forming systems in which growth currents are confined by resistive branches within the advancing pattern are capable of generating the dense branching morphology. We find that in the two- and three-dimensional radial geometries, dissipation and current confinement alone are sufficient to stabilize densely branched growth. However, in the flat geometry, both dissipation in the advancing region and a short diffusion length in the displaced region are necessary to account for stable DBM growth. Our simple yet realistic model predicts the region of parameter space where densely branched growth should be seen. This model provides quantitative predictions for the interfacial velocity as well as for the length scales at which the DBM can appear. We have focused our investigation on the long-wavelength stability of the DBM's envelope, with the understanding that instabilities at short wavelengths are responsible for the finely branched structure of the DBM. Extensions of this model could include consideration of short-wavelength stabilizing mechanisms such as surface tension and terms accounting for the kinetics of attachment. The problem of mode selection for the dense branching morphology then could be addressed.

The photographs in Fig. 1 were produced in collaboration with Len Sander, Roy Clarke, and Nancy Hecker at The University of Michigan. We also are grateful to Peter Garik for pointing out the similarity transform used in Sec. III. This work was supported in part by the MRSEC Program of the National Science Foundation under Contract No. DMR-9400379 and in part by the Petroleum Research Fund of the American Chemical Society under Contract No. 26873-G.

[1] T. A. Witten and L. M. Sander, Phys. Rev. Lett. **47**, 1400 (1981); T. A. Witten and L. M. Sander, Phys. Rev. B **27**, 5686 (1983).

[2] E. Ben-Jacob, P. Garik, T. Mueller, and D. Grier, Phys. Rev. A **38**, 1370 (1988).

[3] Y. Sawada, A. Dougherty, and J. P. Gollub, Phys. Rev. Lett. **56**, 1260 (1986); D. Grier, E. Ben-Jacob, Roy Clarke, and L. M. Sander, *ibid*. **56**, 1264 (1986).

[4] D. G. Grier and D. Mueth, Phys. Rev. E **48**, 3841 (1993).

[5] E. Louis, O. Pla, L. M. Sander, and F. Guinea, Mod. Phys. Lett. B **8**, 1739 (1994).

[6] E. Ben-Jacob and P. Garik, Nature **343**, 523 (1990).

[7] W. W. Mullins and R. F. Sekerka, J. Appl. Phys. **34**, 323 (1963).

[8] D. G. Grier, D. A. Kessler, and L. M. Sander, Phys. Rev. Lett. **59**, 2315 (1987).

[9] D. B. Hibbert and J. R. Melrose, Proc. R. Soc. London A **423**, 149 (1989); J. R. Melrose and D. B. Hibbert, Phys. Rev. A **40**, 1727 (1989).

[10] J. Erlebacher, P. C. Searson, and K. Sieradzki, Phys. Rev. Lett. **71**, 3311 (1993).

[11] P. Garik, R. Zamir, B. Orr, B. Miller, D. Barkey, E. Ben-Jacob, N. Broxholm, and E. Bochner, Phys. Rev. Lett. **62**, 2703 (1989).

[12] Y. Fukunaka, T. Yamamoto, and Y. Kondo, J. Electrochem. Soc. **126**, 3278 (1989).

[13] See, for example, R. M. Brady and R. C. Ball, Nature **309**, 225 (1984); M. J. King and H. Scher, Phys. Rev. A **41**, 874 (1990); V. Frette, K. J. Måløy, F. Boger, J. Feder, and T. Jøsang, Phys. Scr. **T38**, 95 (1991).

[14] A. E. Larsen, D. G. Grier, and T. C. Halsey, Phys. Rev. E **52**, R2161 (1995).

[15] P. Carro, S. L. Marchiano, A. Hernández Creuz, S. González, R. C. Salvarezza, and A. J. Arvia, Phys. Rev. E **48**, R2374 (1993).

[16] C. Zener, J. Appl. Phys. **20**, 950 (1949).